Optimal Prandtl number for heat transfer in rotating Rayleigh–Bénard convection

2010 New J. Phys. 12 075005

(http://iopscience.iop.org/1367-2630/12/7/075005)

New Journal of Physics
The open-access journal for physics

Optimal Prandtl number for heat transfer in rotating Rayleigh–Bénard convection

Richard J A M Stevens[1,4], Herman J H Clercx[2,3] and Detlef Lohse[1]

[1] Department of Science and Technology and JM Burgers Center for Fluid Dynamics, University of Twente, PO Box 217, 7500 AE Enschede, The Netherlands

[2] Department of Applied Mathematics, University of Twente, PO Box 217, 7500 AE Enschede, The Netherlands

[3] Department of Physics and JM Burgers Centre for Fluid Dynamics, Eindhoven University of Technology, PO Box 513, 5600 MB Eindhoven, The Netherlands

E-mail: r.j.a.m.stevens@tnw.utwente.nl

New Journal of Physics **12** (2010) 075005 (8pp)
Received 2 December 2009
Published 8 July 2010
Online at http://www.njp.org/
doi:10.1088/1367-2630/12/7/075005

Abstract. Numerical data for the heat transfer as a function of the Prandtl (Pr) and Rossby (Ro) numbers in turbulent rotating Rayleigh–Bénard convection are presented for Rayleigh number $Ra = 10^8$. When Ro is fixed, the heat transfer enhancement with respect to the non-rotating value shows a maximum as a function of Pr. This maximum is due to the reduced effect of Ekman pumping when Pr becomes too small or too large. When Pr becomes small, i.e. for large thermal diffusivity, the heat that is carried by the vertical vortices spreads out in the middle of the cell and Ekman pumping thus becomes less effective. For higher Pr the thermal boundary layers (BLs) are thinner than the kinetic BLs and therefore the Ekman vortices do not reach the thermal BL. This means that the fluid that is sucked into the vertical vortices is colder than that for lower Pr, which limits the upwards heat transfer.

Turbulent Rayleigh–Bénard (RB) convection, i.e. the flow of a fluid between two parallel plates heated from below and cooled from above, is the paradigmatic system for thermally driven turbulence in a confined space. Considerable progress in understanding the flow dependencies has been achieved in the last two decades, as reviewed in [1, 2]. Here we study the case where the sample is rotated around the vertical axis at an angular velocity, Ω. That system is relevant

[4] Author to whom any correspondence should be addressed.

1367-2630/10/075005+08$30.00

in the astro- and geophysical context, namely for convection in the arctic ocean [3], in the Earth's outer core [4], in the interior of gaseous giant planets [5] and in the outer layer of the Sun [6].

Previous experimental [7]–[13] and numerical studies [11]–[16] at constant Ra and Pr have shown that at moderate rotation rates the convective heat transfer is higher than for the non-rotating case. This heat transport enhancement with respect to the non-rotating case has been ascribed to Ekman pumping [8], [10]–[13], [15]–[18]. Namely, whenever a plume is formed, the converging radial fluid motion at the base of the plume (in the Ekman boundary layer (BL)) starts to swirl cyclonically, resulting in the formation of vertical vortex tubes. The rising plume induces stretching of the vertical vortex tube and hence additional vorticity is created. This leads to enhanced suction of hot fluid out of the local Ekman layer and thus increased heat transport. Corresponding phenomena occur at the upper boundary. This process depends strongly on Ra and Pr [11] and the boundary conditions [19]. Liu and Ecke [7] showed that this increase in Nu can be presented in several ways, as the rotation rate can be expressed by the Taylor Ta number, which measures the effect of the rotational Coriolis force, and the Rossby Ro number, which indicates the relation between the buoyancy and Coriolis forces. Here we choose the latter since Ro indicates when Ekman pumping effects become important with respect to buoyancy effects [12]. In [11] it was shown that no heat transfer enhancement is observed at small $Pr \lesssim 0.7$. This was explained by the larger thermal diffusivity at lower Pr, as a result of which the heat that is carried by the vertical vortices created by Ekman pumping spreads out in the middle of the cell. This leads to a larger destabilizing temperature gradient in the bulk and a lower heat transfer. Furthermore, Ekman pumping turned out to become less effective at higher Ra numbers, where a larger eddy thermal diffusivity limits the effect of Ekman pumping.

In the present work, we systematically determine the heat transfer enhancement with respect to the non-rotating value as a function of the Prandtl (Pr) number by using direct numerical simulations (DNS). We find that in certain regimes the heat flux enhancement can be as large as 30%. Even more remarkably, we observe a hitherto unanticipated maximum in the heat transfer enhancement as a function of Pr.

For a given aspect ratio $\Gamma \equiv D/L$ (D is the cell diameter and L its height) and given geometry (here a cylindrical cell with $\Gamma = 1$), the nature of RB convection is determined by the Rayleigh number $Ra = \beta g \Delta L^3/(\kappa\nu)$ and the Prandtl number $Pr = \nu/\kappa$. Here, β is the thermal expansion coefficient, g the gravitational acceleration, Δ the temperature difference between the bottom and top and ν and κ the kinematic viscosity and the thermal diffusivity, respectively. The rotation rate, Ω, (given in $\mathrm{rad\,s^{-1}}$) is non-dimensionalized in the form of the Rossby number, $Ro = \sqrt{\beta g \Delta/L}/(2\Omega)$. In the DNS we solved the three-dimensional (3D) Navier–Stokes equations within the Boussinesq approximation. The numerical scheme has already been described in [14], [20]–[24]. The numerical details concerning rotating RB convection are described in detail in [11, 12]. Most simulations were performed on a grid of $129 \times 257 \times 257$ nodes, respectively, in the radial, azimuthal and vertical directions, allowing for a sufficient resolution of the small scales both inside the bulk of turbulence and in the BLs (where the grid-point density has been enhanced) for the parameters employed here [11, 12]. Nu is calculated in several ways, as described in detail in [23], and its statistical convergence has been controlled. A grid of $193 \times 385 \times 385$ nodes has been used for the simulations at the highest Pr number and to verify the results for $Pr = 6.4$ obtained on the coarser grid. Furthermore, for the higher Pr number cases the flow is simulated for a very long time (400 dimensionless time units to reach the statistically stationary state followed by 800 time units for

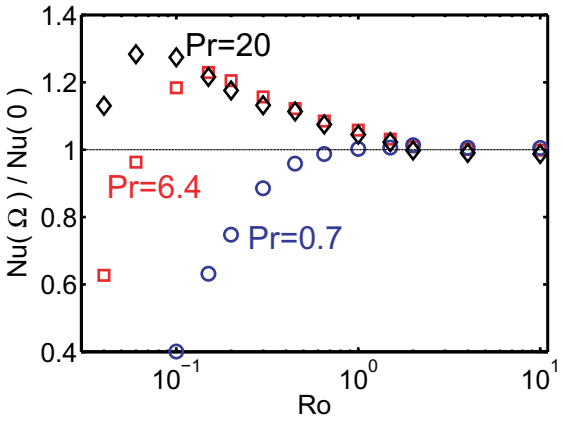

Figure 1. The ratio $Nu(\Omega)/Nu(\Omega = 0)$ as a function of Ro on a logarithmic scale for $Ra = 1 \times 10^8$ and different Pr. Blue open circles, $Pr = 0.7$; red open squares, $Pr = 6.4$; and black open diamonds, $Pr = 20$.

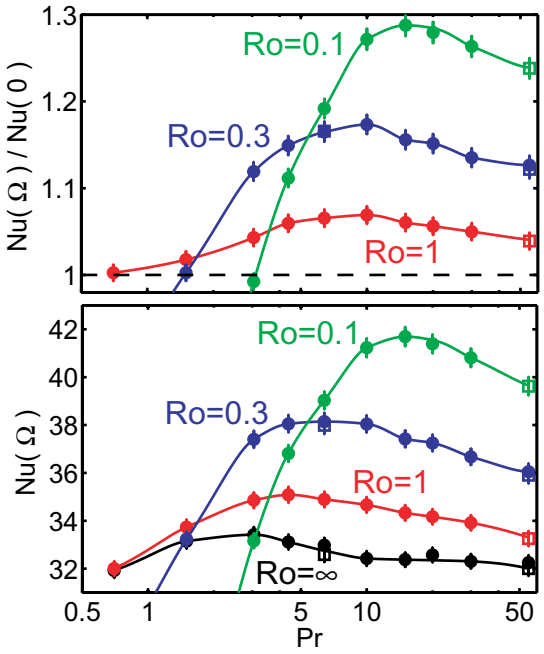

Figure 2. The heat transfer as a function of Pr on a logarithmic scale for $Ra = 1 \times 10^8$. Black, red, blue and green indicate the results for $Ro = \infty$, $Ro = 1.0$, $Ro = 0.3$ and $Ro = 0.1$, respectively. The data obtained on the $193 \times 385 \times 385$ (open squares) and the $129 \times 257 \times 257$ grid (solid circles) are in very good agreement.

averaging) to assure statistical convergence. In [11, 12], we have already shown that our DNS results agree very well with experimental results in this Ra number regime.

The numerical results for $Nu(\Omega)/Nu(0)$ as a function of Ro for several Pr are shown in figure 1. The figure shows that the heat transport enhancement caused by Ekman pumping can be as large as 30% for $Pr = 20$. However, no heat transport enhancement is found for $Pr = 0.7$,

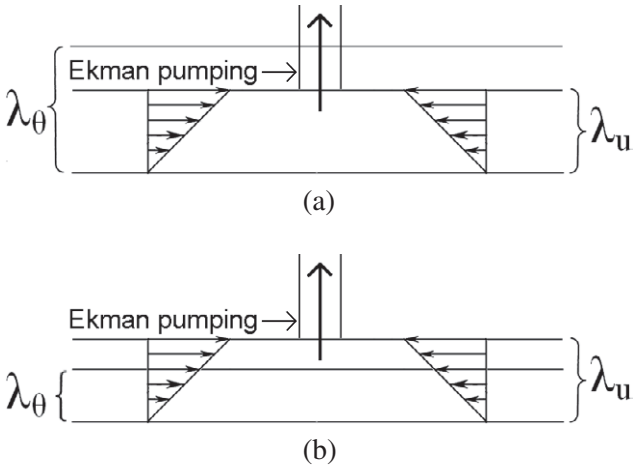

Figure 3. (a) Sketch for the low-Pr number regime where the Ekman vortices reach the thermal BL. (b) Sketch for the high-Pr number regime where the Ekman vortices do not reach the thermal BL.

which is due to the larger thermal diffusivity that makes Ekman pumping less effective [11]. In figure 1, one can already see that the heat transfer enhancement reaches a maximum at a certain Pr when the Ro number is fixed. Indeed figure 2 confirms that the heat transfer enhancement as a function of Pr reaches a maximum. Its location depends on Ro; namely, the stronger the rotation rate the higher the Pr number for which the maximum heat transfer enhancement is found. This trend is even more pronounced when the heat transfer $Nu(Ro)$ itself is considered.

The observation that there is a Pr number for which the heat transfer enhancement is largest suggests that there should be at least two competing effects, which strongly depend on the Pr number, that control the effect of Ekman pumping. There is the question of why Ekman pumping becomes less effective for higher Pr numbers. Clearly, it must have a different origin to the reduced effect of Ekman pumping at lower Pr. Indeed, there is an important difference between the high and the low Pr number regime, namely the relation between the thickness of the thermal and kinetic BLs. For the low Pr number regime the kinetic BL is thinner than the thermal BL and therefore the fluid that is sucked into the vertical vortices is very hot. When the Pr number is too low this heat will spread out in the middle of the cell due to the large thermal diffusivity. For somewhat higher Pr number the fluid that is sucked out of the thermal BL is still sufficiently hot and due to the smaller thermal diffusivity the heat can travel very far from the plate in the vertical vortices. In this way, Ekman pumping can increase the heat transfer for moderate Pr. In the high Pr number regime, the kinetic BL is much thicker than the thermal BL. Therefore, the Ekman vortices forming in the bulk do not reach the thermal BL, and hence the temperature of the fluid that enters the vertical vortices is much lower. This is shown schematically in figure 3.

An investigation of the temperature isosurfaces [11] revealed long vertical vortices, as suggested by Ekman pumping at $Pr = 6.4$, whereas these structures are much shorter and broadened for the $Pr = 0.7$ case due to the larger thermal diffusivity at lower Pr [11]. In figure 4, we show the temperature isosurfaces at $Ro = 0.30$ for several Pr to identify the difference between the high and moderate Pr number cases. The figure reveals that the vertical transport of hot (cold) fluid away from the bottom (top) plate through the vertical vortex tubes is strongly reduced in the high Pr number regime as compared to the case where $Pr = 6.4$. This

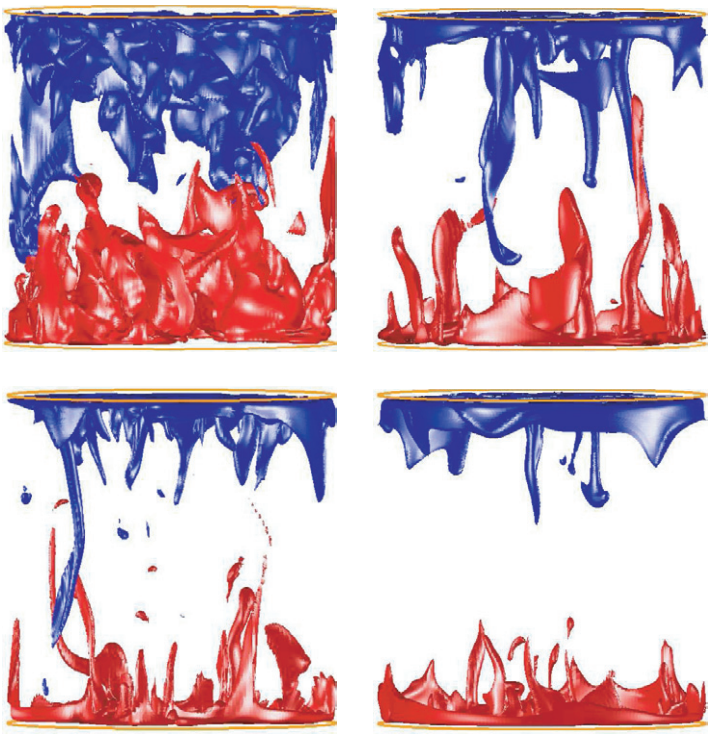

Figure 4. 3D visualization of the temperature isosurfaces in the cylindrical sample of $\Gamma = 1$ at 0.65Δ (red) and 0.35Δ (blue), respectively, for $Pr = 0.7$ (left upper plot) and $Pr = 6.4$ (right upper plot), $Pr = 20$ (left lower plot) and $Pr = 55$ (right lower plot) for $Ra = 10^8$ and $Ro = 0.30$. The snapshots were taken in the respective statistically stationary regimes.

is illustrated in figure 4, where the threshold for the temperature isosurfaces is taken as constant for all cases. Indeed, a closer investigation shows that the vortical structures for the higher Pr are approximately as long as for the $Pr = 6.4$ case. This confirms the view that the temperature of the fluid that is sucked into the Ekman vortices decreases with increasing Pr.

To further verify the above explanation, we determined the horizontally averaged temperature at the kinetic BL height, defined as two times the height where $\epsilon_u'' := \mathbf{u} \cdot \nabla^2 \mathbf{u}$ has its maximum, see [23]–[25] for details. This height is chosen as it indicates the position where the effects of Ekman pumping are dominant. Furthermore, we also determined the horizontally averaged temperature at the edge of the radially dependent thermal BL thickness, i.e. $\lambda_\theta^{sl}(r)$. We determined $\lambda_\theta^{sl}(r)$ by finding the intersection point between the linear extrapolation of the temperature gradient at the plate with the behaviour found in the bulk (see [24]). Indeed, figure 5 shows that the average temperature at the edge of the kinetic BL decreases with increasing Pr. Thus, the temperature of the fluid that enters the vertical vortices decreases with increasing Pr, and this limits the effect of Ekman pumping at higher Pr. Furthermore, the temperature difference with respect to the bottom plate shows that for the non-rotating case the kinetic BL is thinner than the thermal BL when $Pr < 1$, and thicker than the thermal BL when $Pr > 1$. The figure shows that this transition point shifts towards higher Pr when the rotation rate is increased. We note that in [24] we find that the kinetic BL thickness scales with $Ro^{1/2}$, i.e. Ekman BL scaling, when $Ro < 1$. Therefore the cases of $Ro = 0.1$ and $Ro = 0.3$, which

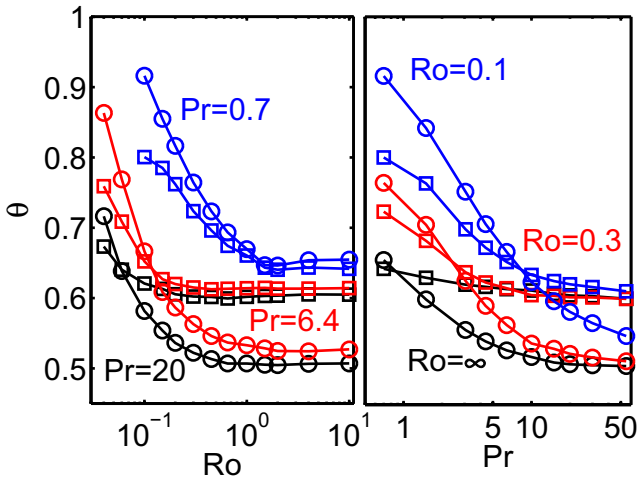

Figure 5. The horizontally averaged temperature at the edge of the kinetic BL (circles) and at the edge of the thermal BL (squares) for $Ra = 1 \times 10^8$. Left: blue, red and black indicates the results for $Pr = 0.7$, $Pr = 6.4$ and $Pr = 20$, respectively. Right: black, red and blue indicate the results for $Ro = \infty$, $Ro = 0.3$ and $Ro = 0.1$, respectively. The results for $Ro = 1$ (not shown) are almost identical to the data obtained for $Ro = \infty$.

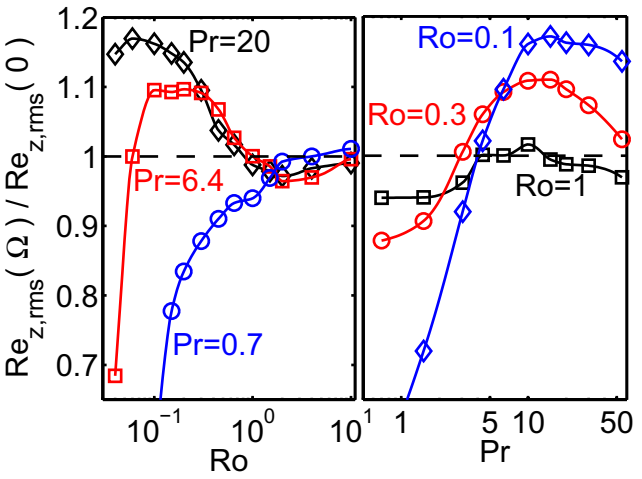

Figure 6. The normalized horizontally averaged rms vertical velocities fluctuation, $Re_{z,rms}$, at the edge of the thermal BL for $Ra = 1 \times 10^8$. Left: blue circles, red squares and black diamonds indicate the data for $Pr = 0.7$, $Pr = 6.4$ and $Pr = 20$, respectively. Right: black squares, red circles and blue diamonds indicate the data for $Ro = 1$, $Ro = 0.3$ and $Ro = 0.1$, respectively.

are shown in figure 5, are in the strong rotating regime where the kinetic BL thickness is approximately equal to the Ekman BL thickness.

Another way to identify the effect of Ekman pumping is to look at the horizontally averaged $Re_{z,rms}$ (dimensionless root mean square (rms) velocity of the axial velocity fluctuations) value at the height $\lambda_\theta^{sl}(r)$ [12]. An increase in the value of $Re_{z,rms}$ shows that Ekman pumping becomes important. In figure 6(b), it is shown that Ekman pumping is strongest for moderate Pr, because

$Re_{z,rms}$ has a maximum around $Pr = 10$. Note that the strength of the Ekman pumping measured in this way reflects the measured Nu number enhancement. One can also deduce from figure 5 that the kinetic BL becomes thinner with respect to the thermal BL when the rotation rate is increased, because the temperature difference with the plate becomes smaller. Therefore more hot fluid is sucked into the vertical vortices and this further supports the Ekman pumping effect for moderate rotation rates where the strongest heat transfer enhancement is observed. Furthermore, the maximum in the heat transfer enhancement, as shown in figure 1, occurs at lower Ro, i.e. stronger rotation, for higher Pr. The breakdown of Nu at low Ro is an effect of the suppression of vertical velocity fluctuations through the strong rotation, which is seen in figure 6(a). Moreover, in figure 6(a) it is shown that the vertical velocity fluctuations are suppressed at higher Ro, i.e. lower rotation rate, when Pr is lower. Furthermore, at low Ro there is experimental [15, 18] and numerical [25] evidence that the vertical component of the vorticity at mid height becomes more symmetric. Near the plates it is positively skewed for $Ro \gtrsim 0.5$, which points to the input of positive vorticity by Ekman pumping. For $Ro \lesssim 0.3$, there is a discrepancy between experimental and numerical measurements of the skewness near the plates, i.e. experiments [18] show that the vorticity distribution becomes more symmetric, while numerical results [25] show a further increase of the positive skewness when Ro is decreased.

To summarize, we studied the Pr number dependence of the heat transport enhancement in rotating RB convection and showed that at a fixed Ro number there is a Pr number for which the heat transfer enhancement reaches a maximum. This is because Ekman pumping, which is responsible for the heat transfer enhancement, becomes less effective when the Pr number becomes too small or too large. At small Pr numbers the effect of Ekman pumping is limited due to the large thermal diffusivity, as a result of which the heat that is sucked out of the BLs rapidly spreads out in the bulk. At high Pr numbers the temperature of the fluid that is sucked into the vertical vortices near the bottom plate is much lower, because the thermal BL is much thinner than the kinetic BL, and therefore the effect of Ekman pumping is lower. Furthermore, the rotation rate for which the heat transfer enhancement reaches its maximum increases with increasing Pr, because the suppression of vertical velocity fluctuations only becomes important at larger rotation rates for higher Pr.

Acknowledgments

We thank R Verzicco for providing us with the numerical code. This work was supported by the Foundation for Fundamental Research on Matter (FOM) and the National Computing Facilities (NCF), both sponsored by NWO. The numerical simulations were performed on the Huygens cluster of SARA in Amsterdam.

References

[1] Ahlers G, Grossmann S and Lohse D 2009 *Rev. Mod. Phys.* **81** 503
[2] Lohse D and Xia K Q 2010 *Annu. Rev. Fluid Mech.* **42** 335
[3] Marshall J and Schott F 1999 *Rev. Geophys.* **37** 1
[4] Glazier J A, Segawa T, Naert A and Sano M 1999 *Nature* **398** 307
[5] Busse F H 1994 *Chaos* **4** 123
[6] Miesch M S 2000 *Sol. Phys.* **192** 59
[7] Liu Y and Ecke R E 2009 *Phys. Rev.* E **80** 036314

[8] Rossby H T 1969 *J. Fluid Mech.* **36** 309
[9] Pfotenhauer J M, Lucas P G J and Donnelly R J 1984 *J. Fluid Mech.* **145** 239
[10] Zhong F, Ecke R E and Steinberg V 1993 *J. Fluid Mech.* **249** 135
[11] Zhong J-Q, Stevens R J A M, Clercx H J H, Verzicco R, Lohse D and Ahlers G 2009 *Phys. Rev. Lett.* **102** 044502
[12] Stevens R J A M, Zhong J-Q, Clercx H J H, Ahlers G and Lohse D 2009 *Phys. Rev. Lett.* **103** 024503
[13] King E M, Stellmach S, Noir J, Hansen U and Aurnou J M 2009 *Nature* **457** 301
[14] Oresta P, Stingano G and Verzicco R 2007 *Eur. J. Mech.* **26** 1
[15] Julien K, Legg S, McWilliams J and Werne J 1996 *J. Fluid Mech.* **322** 243
[16] Kunnen R P J, Clercx H J H and Geurts B J 2008 *Europhys. Lett.* **84** 24001
[17] Vorobieff P and Ecke R E 1998 *Physica* D **123** 153
[18] Vorobieff P and Ecke R E 2002 *J. Fluid Mech.* **458** 191
[19] Schmitz S and Tilgner A 2009 *Phys. Rev.* E **80** 015305
[20] Verzicco R and Orlandi P 1996 *J. Comput. Phys.* **123** 402
[21] Verzicco R and Camussi R 1999 *J. Fluid Mech.* **383** 55
[22] Verzicco R and Camussi R 2003 *J. Fluid Mech.* **477** 19
[23] Stevens R J A M, Verzicco R and Lohse D 2010 *J. Fluid Mech.* **643** 495
[24] Stevens R J A M, Clercx H J H and Lohse D 2010 Boundary layers in rotating Rayleigh–Bénard convection *Phys. Fluids* submitted arXiv:1002.3899
[25] Kunnen R P J, Clercx H J H and Geurts B J 2010 *J. Fluid Mech.* **642** 445